ORIGINAL ARTICLE

Experimental study of a positive surge. Part 2: comparison with literature theories and unsteady flow field analysis

Carlo Gualtieri · Hubert Chanson

Abstract   A positive surge is a unsteady open channel flow resulting from the rapid rise of the free-surface. The phenomenon may be observed in water supply canals and channels as well as in some estuaries during spring tidal conditions. The formation and development of positive surges can be predicted using the method of characteristics and shallow water equations. The paper is the second part of a study presenting the results from new experimental investigations conducted in a large rectangular channel. Detailed unsteady velocity measurements were performed with a high temporal resolution using acoustic Doppler velocimetry and non-intrusive free-surface measurement devices. Several experiments were conducted with the same initial discharge ($Q = 0.060\,\mathrm{m}^3/\mathrm{s}$) and six different gate openings after closure resulting in both non-breaking undular and breaking bores. A comparison between main features of the undular surges with literature theories demonstrated that the experimental data were mostly in agreement with Andersen's theory. The analysis of unsteady flow field including Reynolds stresses confirmed and extended previous findings about positive surge hydrodynamics.

Keywords   Environmental hydraulics · Positive surge · Surge front · Free surface measurements · Instantaneous velocity field · Physical modeling · Undular surges analysis · Unsteady flow field · Reynolds stresses

1 Introduction

A positive surge is a unsteady open channel flow resulting from the rapid rise of the free-surface [1,2]. The phenomenon may be observed in water supply canals and channels as

C. Gualtieri (✉)
Department of Hydraulic, Geotechnical and Environmental Engineering (DIGA), University of Napoli "Federico II", Via Claudio 21, 80125 Napoli, Italy
e-mail: carlo.gualtieri@unina.it

H. Chanson
School of Civil Engineering, The University of Queensland, Brisbane, QLD 4072, Australia
e-mail: h.chanson@uq.edu.au

well as in some estuaries during spring tidal conditions [3]. The formation and development of positive surges can be predicted using the method of characteristics and shallow water equations [1–3]. To date, most physical studies included visual observations and free-surface measurements. They rarely encompassed turbulent velocity data except in a few limited studies [12,13,15].

In this paper and its companion [4], the authors present the results from new experimental works conducted in a large rectangular channel to document flow field and hydrodynamics characteristics in positive surges. In the first paper, the basic flow features of the surges and the analysis of wave height attenuation for the undular surges were presented and discussed. In this paper a comparison between previous theories and experimental data for undular surges is first presented in terms of wave amplitude, wave length and wave steepness. Second, some results about the unsteady flow field including Reynolds stresses are discussed for both undular and breaking surges. Some characteristic trends close to the bed and at larger elevation were seen. Overall this study was aimed at confirming and extending previous findings about hydrodynamics characteristics of a positive surge.

2 Undular surges: wave amplitude, length and steepness

Several theoretical estimates of free-surface undulation characteristics were proposed including studies by Keulegan and Patterson [5], Lemoine [6], Tursonov [7] and Andersen [8]. Lemoine [6] followed the linear wave theory, while Andersen's [8] development was based upon a solution of the Boussinesq equation. These theories provide the wave amplitude a_w and the wave length L_w of the undular surge. These theories assumed that the wave amplitude a_w and the wave length are increasing and decreasing, respectively, with the increasing Froude number of the bore in such a way that the wave steepness a_w/L_w is increasing with Fr, which is defined as [4]:

$$Fr = \frac{V_0 + U}{\sqrt{g\, d_0}} \tag{1}$$

where U is the surge velocity as seen by a stationary observer on the channel bank and positive in the upstream direction, d_0 is the initial flow depth and V_0 is the flow velocity.

Figures 1, 2 and 3 compare a large number of undular surge data to the theories of Keulegan and Patterson [5], Lemoine [6] and Andersen [8] and with previous experimental data, such as those from Favre [9], from Benet and Cunge [10], both model and prototype channels, from Treske [11], from Koch and Chanson [12], from Chanson [13], and from Chanson [14] for smooth bed. Some undular tidal bore observations in Daly River [15], Dee River [16], and Dordogne River [17] are also included. Experimental data of only wave steepness of stationary undular hydraulic jumps are finally added [18,19]. Note that the data from Run 60-7 and Run 60-1 are the average among 23 experiments with the ADV system at different vertical elevation, z.

The data are presented as dimensionless quantities a_w/d_0, L_w/d_0 and a_w/L_w and they are corresponding to the first wavelength. They were obtained from the analysis of surface water profiles recorded by the acoustic displacement meter at $x = 5$ m. Both wave amplitude and wave length were calculated as suggested by Koch and Chanson [12]: that is, the wave amplitude a_w was taken as half of the average wave height of the first wave where the wave height is the difference between the water depth at the first crest and the water depth at the first trough. The wave length L_w was obtained from the arrival times of the first and second crest of the surge.
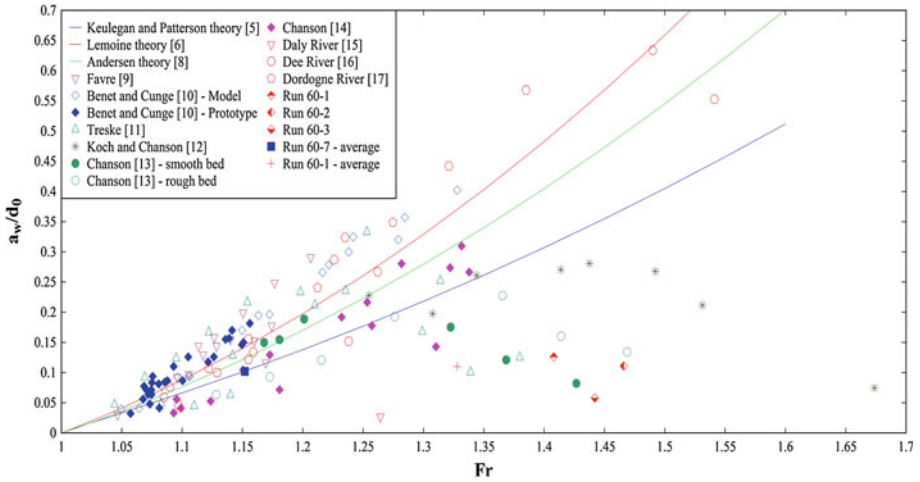
Fig. 1 Dimensionless characteristics of undular bores. Wave amplitude
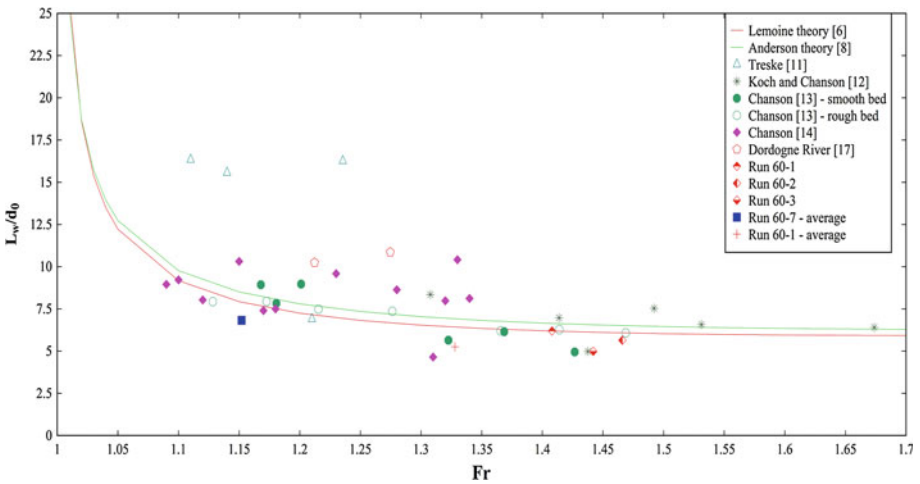
Fig. 2 Dimensionless characteristics of undular bores. Wave length

Figure 1 shows an excellent agreement between Run 60-7 data and previous both theoretical and experimental studies for the same *Fr*. The dimensionless wave amplitude for Run 60-7 close to Keulegan and Patterson [5] theory. For larger Froude numbers, i.e. Run 60-1, 60-2 and 60-3, dimensionless wave amplitude data were lower than the theoretical. Overall, the entire data set, i.e. Run 60-7, Run 60-1, 60-2 and 60-3, followed the same trend as the data of Treske [11] and Koch and Chanson [12], where the wave amplitude decreased sharply immediately before the disappearance of free-surface undulations. It is believed that the flow conditions associated with maximum wave amplitude occurred shortly before the appearance of some wave breaking at the first wave crest [12,14], i.e. for *Fr* in the range from 1.3 to 1.45–1.5 in the present study.
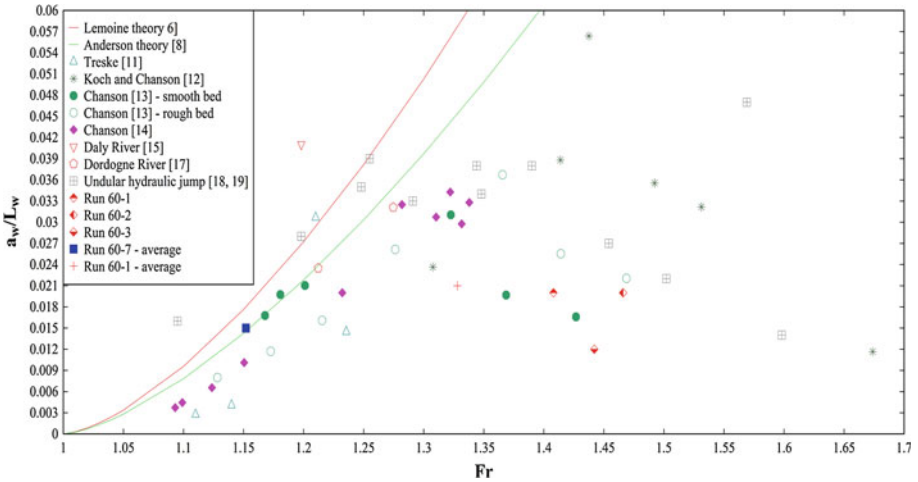
Fig. 3 Dimensionless characteristics of undular bores. Wave steepness

Figure 2 presents some dimensionless wave length data L_w/d_0. All the experimental data were in agreement with both Lemoine and Anderson theories and with the previous literature studies.

Finally Fig. 3 shows the data for wave steepness a_w/L_w. If the averaged data for Run 60-7 was on the Andersen curve, for the remaining experimental data wave steepness exhibited a maximum followed by a sharp decrease for Froude numbers larger than 1.3, which corresponded to the occurrence of some wave breaking at the bore front. This finding was consistent with the trend observed by Koch and Chanson [12] and Chanson [14].

It can be concluded that, in undular surges, both the maximum wave amplitude a_w/d_0 and steepness a_w/L_w were limited by the apparition of light wave breaking at the first wave crest. Second, both Lemoine and Andersen theories resulted in similar values in terms of wave amplitude below $Fr = 1.2$ and in close values of the wave length for all the considered Froude numbers. Third, while the experimental data revealed that Anderson theory, that is based upon the Boussinesq equation, is more accurate when the pressure distribution deviates from hydrostatic, i.e. $Fr = 1.2$–1.5, nevertheless the linear wave theory is simpler in practice and can be applied in engineering problems [14].

3 Unsteady flow field in the surges: results and discussion

For three flow conditions, some detailed velocity measurements were carried out beneath the bore front using the ADV system located at $x = 5$ m (Table 1). Each experiment was repeated to obtain the velocity component time series at several vertical elevations, z. Note that, in Table 1, h_g is the gate opening and the surge front celerity U was calculated using the displacement meters data between $x = 6$ m and 4 m. Also, d_0 was measured at $x = 5$ m and d_{conj} was derived from continuity equation [4]. Note also that details about the ADV system and ADV metrology were provided in the companion paper [4].

Figures 4, 5 and 6 illustrate the effects on the turbulent velocity field at two vertical elevations of three different type of surges, i.e. an undular surge (Run 60-7), an undular surge with some breaking (Run 60-1) and a breaking surge (Run 60-6). Each graph presents the

Table 1 Experimental flow conditions

Run	Q (m³/s)	d_0 (m)	h_g (m)	Type	U (m/s)	d_{conj} (m)	Fr	Remarks
60-1	0.060	0.1387	0.050	Undular	0.777	0.215	1.408	No ADV
60-1	0.060	0.1447	0.050	Undular	0.753	0.209	1.328	ADV measurements
60-2	0.060	0.1396	0.040	Undular	0.857	0.228	1.466	No ADV
60-3	0.060	0.1396	0.025	Undular	0.875	0.231	1.483	No ADV
60-5	0.060	0.1403	0.010	Weak	0.946	0.242	1.536	No ADV
60-6	0.060	0.1369	0.005	Weak	0.911	0.238	1.543	No ADV
60-6	0.060	0.1429	0.005	Weak	0.918	0.237	1.484	ADV measurements
60-7	0.060	0.1427	0.100	Undular	0.519	0.171	1.149	ADV measurements
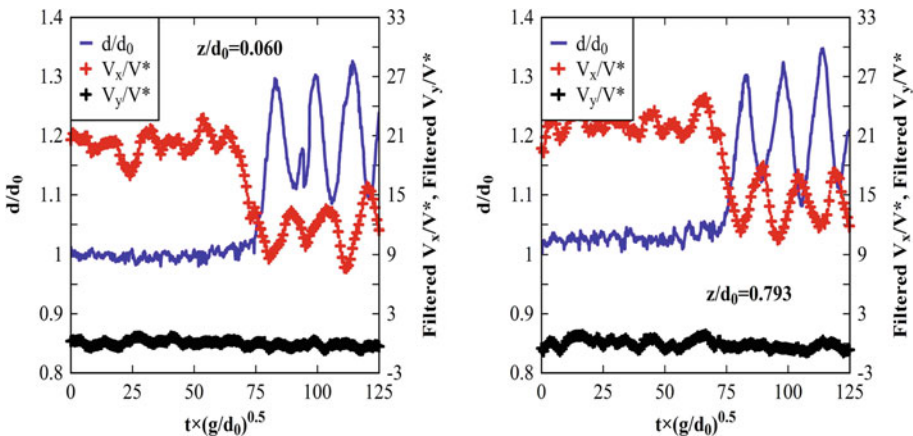
Fig. 4 Undular surge, Run 60-7. Dimensionless instantaneous water depth d/d_0 and velocity components V_x/V^* and V_y/V^* at $z/d_0 = 0.060$ (*left*) and $z/d_0 = 0.793$ (*right*)

dimensionless velocities V_x/V^* and V_y/V^* and water depth d/d_0, where V^* is the shear velocity measured on the channel centerline in steady flow ($V^* = 0.0375$ m/s [4]), against the dimensionless time $t \times (g/d_0)^{0.5}$. Herein V_x is the longitudinal velocity component positive downstream, and V_y is the horizontal transverse velocity component positive towards the left wall. Note that the zero dimensionless time corresponded to 10.0 s prior to the first wave crest passage at the sampling location.

The analysis of experimental velocity data confirmed and extended some basic flow features seen by [12,13] but with a different initial flow rate (see Table 2 in [4]). In the undular surge (Run 60-7), the longitudinal velocity component decreased sharply with the passage of the first wave crest and oscillated with time with the same period as, but out of phase with, the free-surface undulations (Fig. 4). Maximum velocities were observed beneath the wave troughs and minimum velocities below the wave crests. The trend was seen at all vertical locations, and it was consistent with irrotational flow theory which predicts rapid redistributions of velocity distributions between wave crests and troughs, although the latter is based upon the assumption of frictionless fluid. It does not account for bed and sidewall friction, nor for the initial flow turbulence [12]. Note that the streamwise velocities were always positive. In the upper flow region, above $z/d_0 = 0.50$, large fluctuations of transverse, and to some extent longitudinal, velocity components were observed beneath the undulations (Fig. 4). Note that the velocity fluctuation measurements were only an Eulerian characterization of
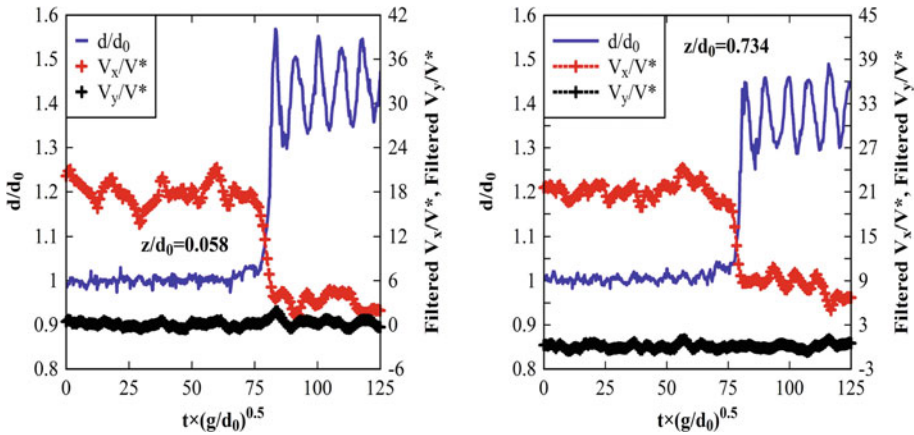
Fig. 5 Undular surge with some breaking, Run 60-1. Dimensionless instantaneous water depth d/d_0 and velocity components V_x/V^* and V_y/V^* at $z/d_0 = 0.058$ (*left*) and $z/d_0 = 0.734$ (*right*)
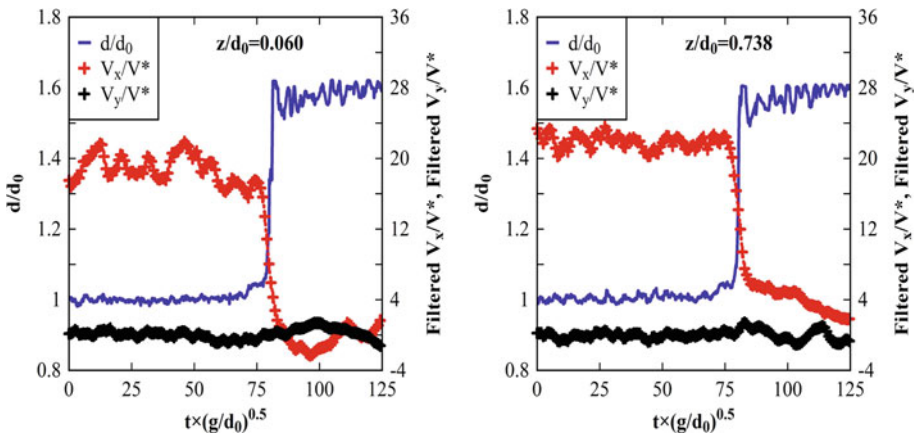
Fig. 6 Breaking surge, Run 60-6. Dimensionless instantaneous water depth d/d_0 and velocity components V_x/V^* and V_y/V^* at $z/d_0 = 0.060$ (*left*) and $z/d_0 = 0.738$ (*right*)

the flow at a fixed position in space. The measured fluctuations included the contributions of the velocity deviation from an ensemble average and the time variation of the ensemble average.

In the undular surge with some breaking (Run 60-1), at both the vertical elevations the streamwise velocity component decreased sharply with the passage of the first wave crest. After that, close to the bed V_x/V^* presented a flat profile (Fig. 5, left), whereas at larger elevation the streamwise velocity component oscillated with time with the same period as, but out of phase with, the free-surface undulations (Fig. 5, right). The amplitude of V_x/V^* were smaller than for the undular surge (Run 60-7).

In the breaking surges, the gentle rise of the free surface was linked to a rapid decrease of the longitudinal velocity component at all vertical elevations. Immediately after, the passage of the roller was marked by a sharp rise in free-surface elevation corresponding to a discontinuity in terms of the water depth. The sudden increase in water depth corresponded to a rapid deceleration to yield a slower flow motion to satisfy the conservation of mass (Fig. 6).

The rate of flow deceleration was notably sharper in a breaking bore than that for an undular bore at the same relative elevation z/d_0 (Figs. 4, 6, left).

Second, the velocity records showed some marked difference depending upon the vertical elevation z (Fig. 6). At the larger depth, i.e. $z/d_0 > 0.3$, the streamwise velocity component decreased rapidly at the surge front but remained positive beneath the roller toe (Fig. 6, right). In contrast, for $z/d_0 < 0.3$, some negative V_x values were observed although for a short duration, for a dimensionless time $t \times (g/d_0)^{0.5}$ from 86 to 106 (Fig. 6, left). The existence a sudden longitudinal flow reversal indicated unsteady flow separation beneath the surge front. The longitudinal flow deceleration yielded negative streamwise V_x velocities with $(V_x/V^*)_{min} = -2.35$. This flow feature was first reported by Koch and Chanson [12] and Chanson [13] and obtained numerically by Furuyama and Chanson [20].

For all experiments, the turbulent velocity data showed some large fluctuations of all velocity components beneath the surge and in the flow field behind the surge. Large time variations of the longitudinal and transverse velocity components were seen at all vertical elevations for both undular and breaking bores. Overall, these experimental results mostly confirmed and extended previous observation for both undular and breaking surges at different flow rates [12,13].

3.1 Reynolds stresses

Figures 7 and 8 present some Reynolds stresses data for Run 60-7 at $z/d_0 = 0.060$, i.e. near the bed, and at $z/d_0 = 0.793$. Large turbulent stresses could be noted below the surge front and ensuing undulations. In particular, intense normal stresses and tangential stresses were consistently seen beneath wave crests and just before each crest (see arrows in Fig. 7, right and left). These turbulent stresses were larger than beneath the following wave troughs. At higher sampling location, i.e. $z/d_0 = 0.793$, a similar trend was observed with larger values of both normal and tangential Reynolds stresses. Overall these trends were consistent with previous literature data [12,13], but the values of both normal and tangential Reynolds stresses were larger than previous observation with a lower flow rate.

The data from the undular surge with some breaking (Run 60-1) were similar to those from the undular surge but they showed a lower link with free surface undulations.
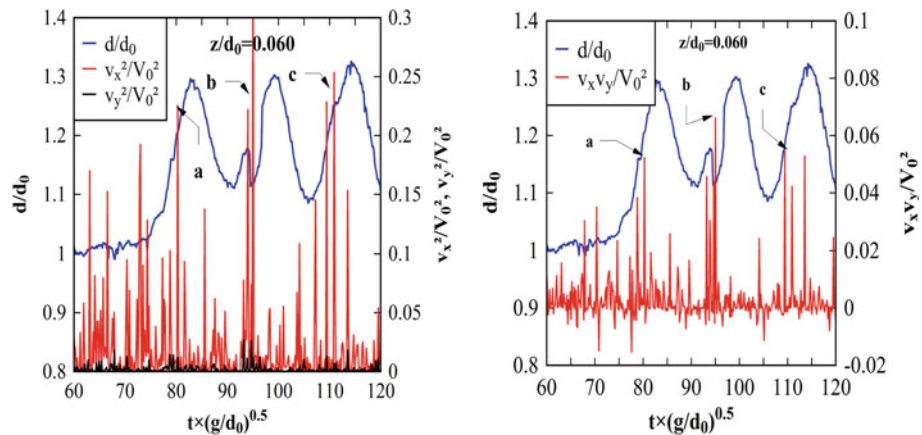
Fig. 7 Undular surge, Run 60-7. Dimensionless instantaneous water depth d/d_0 and normal Reynolds stresses v_x^2/V_0^2 and v_y^2/V_0^2 (*left*) and tangential Reynolds stresses $v_x v_y/V_0^2$ (*right*) at $z/d_0 = 0.060$
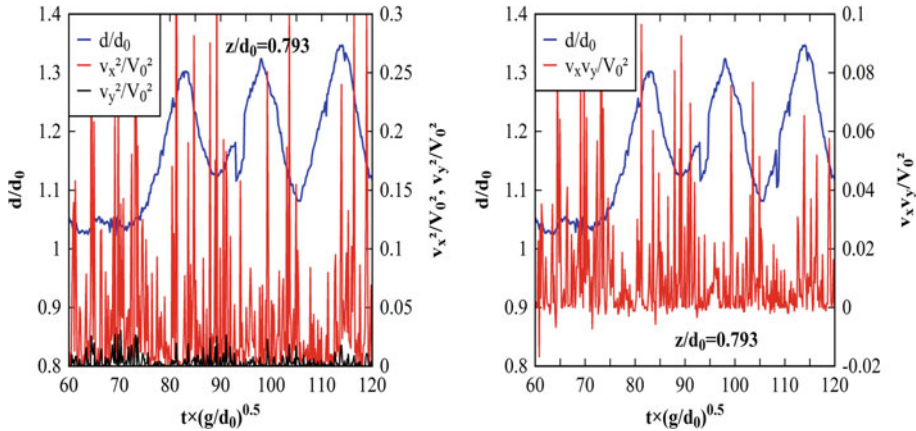
Fig. 8 Undular surge, Run 60-7. Dimensionless instantaneous water depth d/d_0 and normal Reynolds stresses v_x^2/V_0^2 and v_y^2/V_0^2 (left) and tangential Reynolds stresses $v_x v_y/V_0^2$ (right) at $z/d_0 = 0.793$
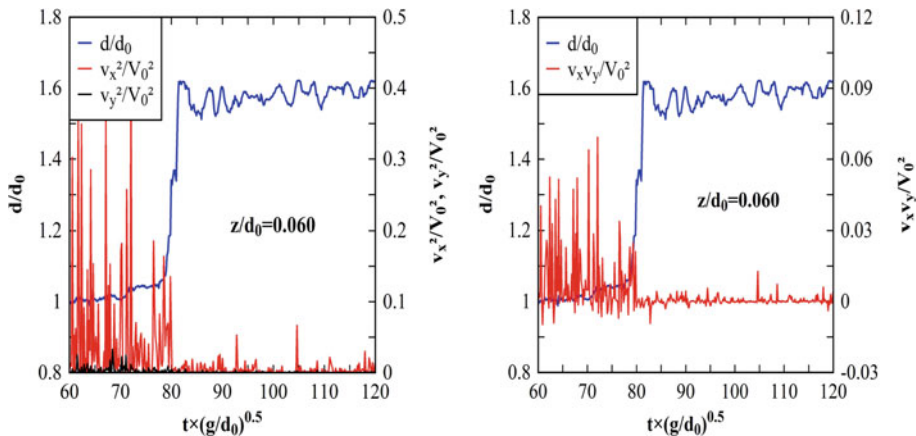
Fig. 9 Breaking surge, Run 60-6. Dimensionless instantaneous water depth d/d_0 and normal Reynolds stresses v_x^2/V_0^2 and v_y^2/V_0^2 (left) and tangential Reynolds stresses $v_x v_y/V_0^2$ (right) at $z/d_0 = 0.060$

Finally, the breaking surge data (Run 60-6) showed large Reynolds stresses below the surge front and roller for $z/d_0 = 0.060$ and $z/d_0 = 0.812$ (Figs. 9, 10). Both normal and tangential stresses were larger than those in the initial steady flow at each sampling point.

Close to the bed (Fig. 9), normal stresses were larger than at higher sampling points. Also, large Reynolds stresses were observed at the passage of the surge roller until $t \times (g/d_0)^{0.5} \approx 85$, followed by lower values. This is consistent with previous findings [12].

The effect of the passage of the roller was more marked at $z/d_0 > 0.5$ (Fig. 10). Large normal stresses v_y^2/V_0^2 were recorded below the surge roller (Fig. 10, left). This result was consistent with large transverse velocity fluctuations recorded beneath the roller toe (Fig. 6, right). Also, at $z/d_0 = 0.815$ tangential Reynolds stresses larger than close to the bed were observed below the surge until $t \times (g/d_0)^{0.5} \approx 90$ (Figs. 9, 10, right). It is believed that the sudden increase in normal and tangential turbulent stresses for $0.5 < z/d_0 < 1$ was caused by the developing mixing layer of the roller [12]. Note that in present study, no sampling
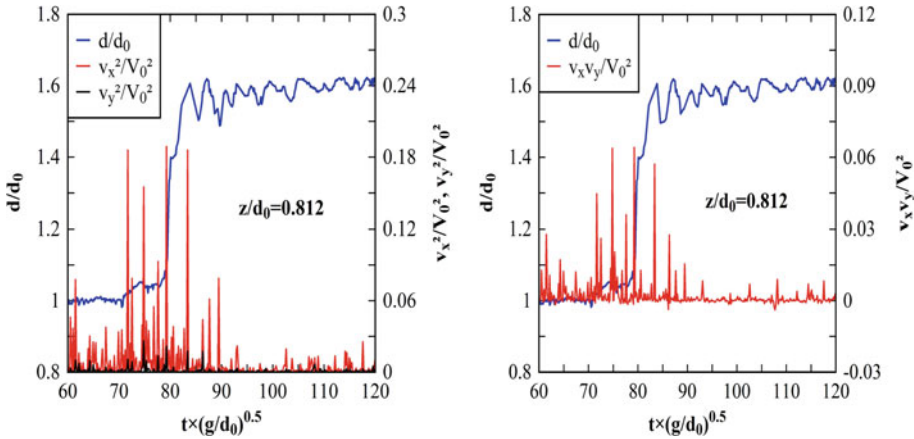
Fig. 10 Breaking surge, Run 60-6. Dimensionless instantaneous water depth d/d_0 and normal Reynolds stresses v_x^2/V_0^2 and v_y^2/V_0^2 (*left*) and tangential Reynolds stresses $v_x v_y/V_0^2$ (*right*) at $z/d_0 = 0.812$

could be conducted for $z/d_0 > 1$ and there was no turbulence data in the surge roller itself. Overall, the results for the weak surge were consistent with previous experimental findings [12,13].

4 Conclusion

This study presented some physical measurements in positive surges conducted under controlled flow conditions in a large channel. Detailed turbulence measurements were performed with a high-temporal resolution (50 Hz) using side-looking acoustic Doppler velocimetry and non-intrusive free surface measurement devices. Using the same initial flow conditions, several experiments were performed with non-breaking and breaking surges propagating upstream against the initially steady flow. The dependant variable was the downstream gate opening after closure. Both undular and breaking surges were observed depending upon the surge Froude number. The range of Froude numbers corresponding to each type of surge was consistent with previous literature findings.

The experimental data for wave amplitude, wave length and wave steepness for the undular surges were compared to the theoretical solutions of Keulegan and Patterson [5], Lemoine [6] and Anderson [8]. The wave length data were generally in agreement with both Lemoine's and Andersen's theories, while the wave steepness data were mostly close to Andersen's theory, based upon a solution of the Boussinesq equation. The wave amplitude data were in the range of values predicted from the above theories. However both the maximum wave amplitude a_w/d_0 and steepness a_w/L_w were limited by the apparition of wave breaking at the first wave crest. The amplitude and steepness data exhibited a sharp decrease above $Fr = 1.3$, when some breaking was observed at the surge front.

Detailed instantaneous velocity measurements showed a marked effect of the surge passage. In the undular surges, the streamwise velocity component decreased sharply with the passage of the first wave crest and oscillated with time with the same period as, but out of phase with, the free-surface undulations. Also, the streamwise velocity component was always positive. The same trend was observed for the undular surge with some breaking, but

the streamwise velocity component data exhibited undulations smaller than in the undular surge and close to the bed they had a flat profile. In the breaking surge, the gentle rise of the free surface corresponded to a rapid flow deceleration at all vertical elevations, and some flow reversal were measured next to the bed, whereas at highest sampling points V_x / V^* remained positive.

The analysis of instantaneous velocity data also provided Reynolds stresses. Large Reynolds stresses were observed for both undular and breaking surges. In the undular surge, turbulent stresses were larger beneath wave crests and just before each crest, than below the following wave troughs. In the breaking surge, large Reynolds stresses were observed below the surge front and roller at all the sampling elevations. At the highest elevations, large transverse normal stresses below the surge roller and intense tangential stresses for a prolonged time beneath the surge were recorded.

Overall this study, including [4], provided a comprehensive survey of the characteristics of non-breaking undular and breaking surges. The results mostly confirmed and extended the main findings of previous experimental works.

References

1. Henderson FM (1966) Open channel flow. MacMillan Company, New York
2. Chanson H (2004) The hydraulics of open channel flows: an introduction, 2nd edn. Butterworth-Heinemann, Oxford
3. Chanson H (2011) Current knowledge in tidal bores and their environmental, ecological and cultural impacts. Environ Fluid Mech 11(1):77–98. doi:10.1007/s10652-009-9160-5
4. Gualtieri C, Chanson H (in press) Experimental study of a positive surge. Part 1: basic flow patterns and wave attenuation. Environ Fluid Mech. doi:10.1007/s10652-011-9218-z
5. Keulegan GH, Patterson GW (1940) Mathematical theory of irrotational translation waves. Journal of Research of the National Bureau of Standards, RP1273, US Dept. of Commerce. 24(1):47–101
6. Lemoine R (1948) Sur les ondes positives de translation dans les canaux et sur le ressaut ondulé de faible amplitude (On the Positive Surges in Channels and on the Undular Jumps of Low Wave Height). La Houille Blanche, Mar–Apr., pp 183–185 (in French)
7. Tursunov AA (1969) Subtrical State of Free-Surface Flows. Izv. Vsesoyuz. Naucho-Issled. Inst. Gidrotekh., Vol 90, pp 201–223 (in Russian). (Also known as : Tursanov AA (1969) Free-Surface Flow States at the Neighbourhood of Critical Flow Proc VNIIG, Vol 90, pp 201–223 (in Russian)
8. Andersen VM (1978) Undular Hydraulic Jump. Jl of Hyd. Div., ASCE, Vol 104, No. HY8, pp 1185–1188. Discussion: Vol 105, No. HY9, pp 1208–1211
9. Favre H (1935) Etude théorique et expérimentale des ondes de translation dans les canaux découverts (Theoretical and experimental study of travelling surges in open channels). Dunod, Paris, France (in French)
10. Benet F, Cunge JA (1971) Analysis of experiments on secondary undulations caused by surge waves in trapezoidal channels. J Hydraul Res IAHR 9(1):11–33
11. Treske A (1994) Undular bores (Favre-waves) in open channels—experimental studies. J Hydraul Res, IAHR 32(3):355–370. Discussion: 33(3):274–278
12. Koch C, Chanson H (2009) Turbulence measurements in positive surges and bores. J Hydraul Res 47(1):29–40
13. Chanson H (2010) Unsteady turbulence in tidal bores: effects of bed roughness. J Waterway Port Coast Ocean Eng 136(5):247–256
14. Chanson H (2010) Undular tidal bores: basic theory and free-surface characteristics. J Hydraul Eng ASCE 136(11):940–944
15. Wolanski E, Williams D, Spagnol S, Chanson H (2004) Undular tidal bore dynamics in the Daly Estuary, Northern Australia. Estuar Coast Shelf Sci 60(4):629–636
16. Lewis AW (1972) Field Studies of a Tidal Bore in the River Dee. M.Sc. thesis, Marine Science Laboratories, University College of North Wales, Bangor, UK
17. Navarre P (1995) Aspects physiques du caractere ondulatoire du Macaret en Dordogne (Physical features of the undulations of the Dordogne River tidal bore). D.E.A. thesis, Univ. of Bordeaux, France (in French)

18. Montes JS, Chanson H (1998) Characteristics of undular hydraulic jumps. Results and calculations. J Hydraul Eng 124(2):192–205
19. Chanson H (2005) Physical modelling of the flow field in an undular tidal bore. J Hydraul Res 43(3):234–244
20. Furuyama S, Chanson H (2008) A numerical solution of a tidal bore flow. Coast Eng J 52(3):215–234